bility"). In other words, Flower and Linnhoff's equation counts a number of networks which contain both cycles and unmatched streams, as the authors recognize. Of course, when a problem has only one utility, as is frequently the case, no trees involving hot utility-cold utility matches are counted by Eq. 3.

LITERATURE CITED

Flower, J. R., and B. Linnhoff, "A Thermodynamic-Combinatorial Approach to the Design of Optimal Heat-Exchanger Networks," *AIChE J.*, **26**, No. 1, 1 (1980).

Hohmann, E. C., "Optimum Networks for Heat Exchange," Ph.D. Thesis, Univ. S. Calif. (1971).

Linnhoff, B., D. Mason, and I. Wardle, "Understanding Heat Exchanger Networks," *Comp. in Chem. Eng.*, **3**, 295 (1979).

Linnhoff, B., and J. A. Turner, "Simple Concepts in Process Synthesis Give Energy Savings and Eleqant Designs," *The Chem. Eng.*, 742 (Dec., 1980).

Nishida, N., G. Strephanopoulos, and A. W. Westerberg, "A Review of Process Synthesis," *AIChE J.*, **27**, No. 3, 321 (1981).

Scoins, H. I., "The Number of Trees with Nodes of Alternate Parity," *Proc. Cambridge Phil. Soc.*, **58**, 12 (1962).

Manuscript received October 18, 1982, and accepted April 15, 1983.

Gas Transport within the Developed Pore Structure of Reactive Porous Matrices

TEVFIK BARDAKCI

Department of Chemical Engineering
The Catholic University of America
Washington, DC 20064

and

L. L. GASNER

Department of Chemical Engineering
University of Maryland
College Park, MD 20742

INTRODUCTION

Heterogeneous gas-solid reactions where the reactive solid surfaces exist in micropores throughout solid pellets are commonplace to chemical engineers. A common observation is that the reactivity of an individual pellet varies with time. Indeed, at very high temperatures individual pellets internally melt and "deadburn," thereby totally eliminating internal microporous reactivity. This sintering phenomenon may also occur to lesser extents at lower reaction temperatures and would be expected to be most important for relatively high temperature reactions. One particular example of a high temperature reaction is sulfur dioxide capture by calcined calcium carbonate (limestone or dolomite) in fluidized bed combustion.

This paper presents experimental measurements of effective diffusivity of inert gases through a reactive porous matrix as a function of time and temperature. An empirical correlation is obtained which should be of value in modeling heterogeneous chemical reactions and in understanding the mechanisms of the changes in internal micropore structure. Previous studies have measured effective diffusivity at a single time and, therefore, have neglected this sintering phenomenon.

The system chosen is that of a natural calcium carbonate limestone which first decomposes, called calcination, giving off 44% of the $CaCO_3$ weight as CO_2 and yielding a reactive matrix of microporous calcium oxide with a porosity of about 0.45. Calcination dissociation proceeds gradually from the outside surface of the individual particle inward (Boynton, 1966). The developed mircoporous structure is reactive to acidic gas components such as SO_2, H_2S and CO_2.

Other investigators have studied this system but all used reactive CO_2 rather than an inert gas in their study, and none studied the system as a function of time. Campbell et al. (1970) fabricated *individual* particles from powdered $CaCO_3$ in a press. After calcination they found that the effective diffusivity of CO_2 through porous CaO ranged from 0.08 to 0.28 $cm^2 \cdot s^{-1}$ for porosities of 0.4–0.8 for temperatures between 870 and 950°C. They concluded that Knudsen diffusion predominated. Hills (1968) obtained the following empirical correlation for the effective diffusivity of CO_2 through porous CaO:

$$D_e = a + b(T - 1{,}103.15) \tag{1}$$

where $a = 0.083 \pm 0.002\ cm^2 \cdot s^{-1}$, $b = 0.000210 \pm 0.000003\ cm^2 \cdot s^{-1} \cdot K^{-1}$, and T is the calcination temperature. Satterfield (1970) combined the Knudsen equation with the parallel pore model to obtain the following equation to estimate the effective diffusivity of gases through porous solids:

$$D_e = 19{,}400 \frac{\epsilon^2}{\tau S_g \rho_p} \sqrt{\frac{T}{M}} \tag{2}$$

EXPERIMENTAL METHOD

A cylindrical pellet (typically 0.31cm thick by 2.1 cm diameter) was manufactured using a diamond coring drill bit and a carborundum saw The limestone used (Greer Limestone Co., Morgantown, WV) had an average calcium carbonate content of 75%. This pellet was mounted in a specially designed high temperature diffusion cell (Bardakci, 1980, Bardakci and Gasner, 1981) using the same principle as that of Wicke and Kallenbach (1941). The diffusion cell reactor was mounted in a tube furnace which was controlled to a selected fixed temperature. Argon gas flowed radially across one face of the pellet while nitrogen gas flowed radially across the other face. The temperature was measured at each pellet face. The differential pressure between the two sides of the pellet was maintained at 0.00 ± 0.03 cm. of water by computer control. The computer also measured and controlled flow rates and absolute pressure of each stream. In addition, it automatically injected samples from each stream into a gas chromatograph, integrated the output, and calculated many things including the effective diffusivity of argon and nitrogen through the reactive microporous pellet.

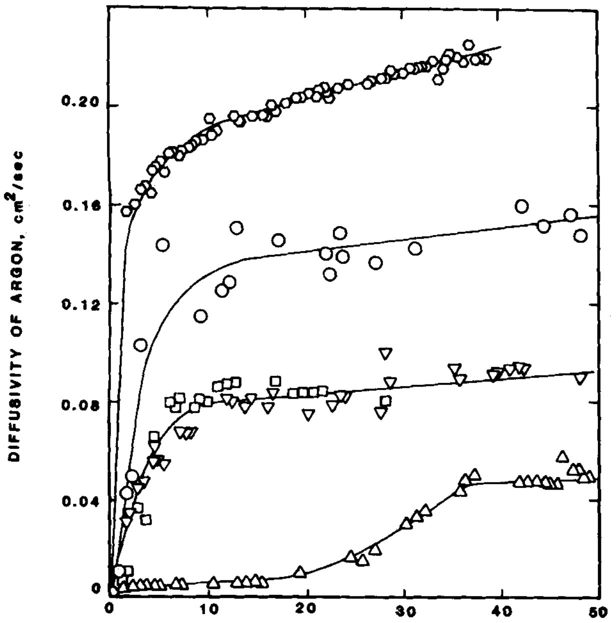

Figure 1. Effective diffusivity of argon as a function of time. ⬡ 1,239K, ○ 1,215K, ▽ 1,120K, □ 1,114K, △ 1,029K.

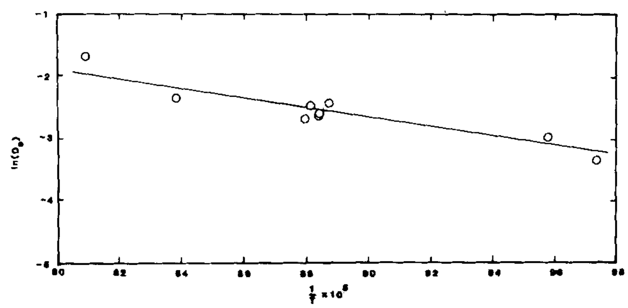

Figure 2. Arrhenius plot of D_o.

RESULTS AND DISCUSSION

Before calcination the pellet was nonporous in that no flux of either diffusing gas could be detected. Effective diffusivities of argon and nitrogen through the developing microporous calcining pellet was measured as a function of calcination time at different fixed temperatures. It was found that the effective diffusivity continued to increase after calcination was complete. This is attributed to a sintering type of microcrystal rearrangement within the constant dimension pellet which resulted in this increasing gas flux. This paper presents basic data and empirical correlation of this phenomenon.

The effective diffusivity of argon as a function of calcination and sintering time at various temperatures is shown in Figure 1. The lowest temperature data show a sigmoidal shape not evident at higher temperatures. This is due to the extremely long time required to calcine the pellet completely, 36.5 h, in contrast to the relatively short time required at higher temperatures.

The data were fit to an empirical (2 constant) straight line mathematical form. The constants obtained are the slope, S, here called the sintering constant, and the extrapolated intercept, D_o, which is a pseudoeffective diffusivity at zero hours of sintering. The general form of the equation is as follows:

$$D_e^{Ar} = D_o + S\theta \tag{3}$$

where D_e^{Ar} is the effective diffusivity for argon in cm²/s. Table 1 shows the best fit equations for each several experimental runs at several temperatures.

It was found that these constants varied with temperature according to an Arrhenius-type relationship as follows:

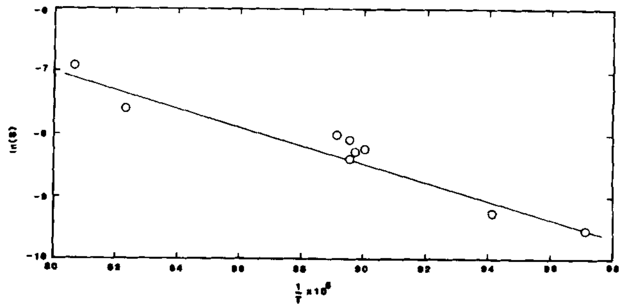

Figure 3. Arrhenius plot of sintering constant.

TABLE 1. EFFECTIVE DIFFUSIVITY CORRELATION RESULTS

Run No.	Temp., K	Best Fit Equation
C1	1,116	$D_e = 0.091 + 0.000237\ \theta$
C2	1,062	$D_e = 0.072 + 0.000092\ \theta$
C3	1,239	$D_e = 0.182 + 0.001001\ \theta$
C5	1,111	$D_e = 0.098 + 0.000266\ \theta$
C6	1,116	$D_e = 0.089 + 0.000315\ \theta$
C7	1,120	$D_e = 0.075 + 0.000323\ \theta$
C8	1,215	$D_e = 0.131 + 0.000480\ \theta$
C9	1,029	$D_e = 0.043 + 0.000071\ \theta$
C12	1,114	$D_e = 0.078 + 0.000250\ \theta$

$$D_o = A_o e^{-E_D/RT} \tag{4}$$

and

$$S = A_1 e^{-E_S/RT} \tag{5}$$

Figures 2 and 3 show the values of D_o and S from Table 1 on an Arrhenius plot. It can be seen that this form is approximately valid. The preexponential terms were found to be A_o = 62.32 cm·s^{-1} and A_1 = 113.7 cm^2·s^{-1}·h^{-1}, respectively. The activation energies were found to be E_D = 14,600 cal·gmol^{-1} and E_S = 29,200 cal·gmol^{-1}, respectively. The best empirical fit to all the data then becomes:

$$D_e^{Ar} = 62.32e^{-14,600/RT} + 113.7e^{-29,200/RT} \cdot \theta \tag{6}$$

This equation can be used to estimate the effective diffusivity of reactive gases through the internal microporous reactive structures of pellets from the particular source used. It would be expected that pellets from other sources would yield individual constants that are somewhat different, yet this correlation should be useful in modeling heterogeneous chemical reactions of various types. It should be noted that the data agree with the results of Campbell et al. (1970) and of Hills (1968); however, this earlier work did not include measurements as a function of both time and temperature. Also, this correlation can be extended to other gases by multiplying by the reciprocal square root of the molecular weight ratio (Evans et al., 1961). A further observation is that both high values of activation energy observed are much higher than expected activation energies for gaseous diffusion alone, therefore, chemical reactions involving chemical bond breaking and chemical rearrangements within crystals are indicated.

NOTATION

a = constant in Eq. 1, cm^2·s^{-1}
A_o = constant in Eq. 4, cm^2·s^{-1}
A_1 = constant in Eq. 5, cm^2 · s^{-1} · hr^{-1}
b = constant in Eq. 1, cm^2 · s^{-1} · K^{-1}
D_e^{Ar} = effective diffusivity of argon, cm^2 · s^{-1}
D_o = intercept in Eq. 3, cm^2 · s^{-1}
E_D = activation energy in Eq. 4, cal · gmol^{-1}
E_S = activation energy in Eq. 5, cal · gmol^{-1}
M = molecular weight, g · gmol^{-1}
S = sintering constant, cm^2 · s^{-1} · h^{-1}
S_g = specific surface area, cm^2 · g^{-1}
T = calcination and sintering temperature, K

Greek Letters

ϵ = porosity
ρ = density, $g \cdot cm^{-3}$
τ = tortuosity factor
θ = calcination and sintering time, h

LITERATURE CITED

Bardakci, T., and L. L. Gasner, "Experimental Studies Using a Single Pellet High Temperature Duffusion Cell Reactor," *Thermochimica Acta*, **45**, 233 (1981).

Bardakci, T., "Heterogeneous-Gas Solid Reaction Studies in a High Temperature Diffusion Cell: The Effect of Sodium Chloride on Sulfur Capture in Fluidized Bed Combustion," Ph.D. Thesis, University of Maryland (1980).

Boynton, R. S., *Chemistry and Technology of Lime and Limestone*, John Wiley and Sons, New York (1966).

Campbell, F. R., and A. W. D. Hills, and A. Paulin, "Transport Properties of Porous Lime and Their Influence on the Decomposition of Porous Compacts of Calcium Carbonate," *Chem. Eng. Sci.*, **25**, 929 (1970).

Evans, R. B., G. M. Watson, and E. A. Mason, "Gaseous Diffusion in Porous Media at Uniform Pressure," *J. Chem. Phys.*, **35**, 2076 (1961).

Hills, A. W. D., "The Mechanism of the Thermal Decomposition of Calcium Carbonate," *Chem. Eng. Sci.*, **23**, 297 (1968).

Satterfield, C. N., *Mass Transfer in Heterogeneous Catalysis*, M.I.T. Press, Cambridge, MA (1970).

Wicke, E., and R. Kallenbach, "Counter-Diffusion Through Porous Pellet," *Kolloid* Z., **97**, 135 (1941).

Manuscript received December 9, 1982; revision received January 24, and accepted January 31, 1983.

Solids Mixing in a Gas-Liquid-Solid Fluidized Bed Containing a Binary Mixture of Particles

LIANG-SHIH FAN, S. H. CHERN,
and K. MUROYAMA

Department of Chemical Engineering
The Ohio State University
Columbus, OH 43210

In the practical application using a gas-liquid-solid fluidized bed for chemical or biochemical processing, a size distribution of the solid particles in the bed is commonly encountered. Particle stratification or segregation would occur in the bed, should adequate mixing among particles not be established. This note describes the experimental efforts on the investigation of the solids mixing in a three-phase fluidized bed containing a binary mixture of particles. Qualitative analysis of the mixing states including complete segregation, partial intermixing, and complete intermixing is conducted.

EXPERIMENTAL

The schematic diagram of the experimental apparatus is shown in Figure 1. The vertical Plexiglas column in the figure has the dimension of 76.2 mm ID with a maximum height of 2.730 m. The column consists of three sections: the gas-liquid disengagement section, test section, and gas-liquid distsributor section. The gas-liquid distributor, which is located at the bottom of the test section, is designed in such a manner that uniform distributions of liquid and gas can be maintained in the column (Fan et al., 1982).

Water and air were used as the liquid and gas phases in the experiment. The gas-liquid flow is cocurrent and upward. Calibrated rotameters were used for the measurement of the gas and the liquid flow rates. Pressure taps are evenly spaced at 51 mm intervals axially on the wall of the test section. The pressure taps were connected to water manometers for the measurement of the static pressure gradient along the column.

In each experiment, two sizes of glass particles were used. The small particles were colored with black paint (Dean and Barry, A-23, wrought iron-flat paint) while the large particles were colored with white paint (Krylon, flat paint). The colored particles were well premixed before placing in the column. Two binary mixtures, including the mixture of 3 and 4 mm particles, and that of 3 and 6 mm particles, are considered in this study. The weight ratio of each size of the particles in the mixture is 1:1.

RESULTS AND DISCUSSION

The qualitative analysis of the solids mixing based on visual observation is presented. Three states of solids mixing are classified in the experiment. These states are complete segregation, partial intermixing, and complete intermixing. It should be noted that although the classification of the states may be to some extent

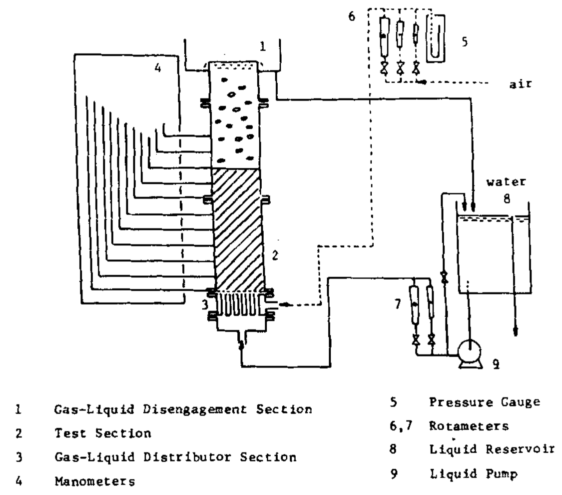

Figure 1. Schematic diagram of the experimental apparatus for the study of solids mixing in a gas-liquid-solid fluidized bed containing a binary mixture of particles.

Correspondence concerning this paper should be addressed to L. S. Fan.

K. Muroyana is on leave from the Department of Environmental Chemistry and Technology, Tottori University, Tottiri, Japan